25th International Congress on Sound and Vibration
8-12 July 2018 HIROSHIMA CALLING
ICSV25

PSYCHOACOUSTIC HYBRID ACTIVE NOISE CONTROL STRUCTURE FOR APPLICATION IN HEADPHONES

Piero Rivera Benois and Udo Zölzer
Helmut Schmidt University, Department of Signal Processing and Communications, Hamburg, Germany
email: piero.rivera.benois@hsu-hh.de

Veatriki Papantoni
German Aerospace Center (DLR), Institute of Composite Structures and Adaptive Systems, Braunschweig, Germany

Psychoacoustic active noise control aims to decrease the perceived loudness and annoyance of the acoustic noise present in the environment. In order to achieve this, the frequencies to which the human ear is more sensitive are attenuated with higher priority. An implementation of such a control system based on FeLMS and noise weighting curves has shown to effectively improve the pleasantness of the residual noise. However, although it produces attenuation within the critical frequency region, the high frequencies are partially amplified and the low frequencies remain almost unaltered. In this paper, a hybrid structure is proposed for the application in active noise control headphones, which extends the attenuation capabilities of the feedforward control structure with a decoupled classical feedback controller. The feedback controller is designed to attenuate the residual error in the low-frequency region, thus partially compensating the limitations of the original structure. A real-time FPGA implementation of the proposed hybrid control structure is presented and its performance is evaluated based on measurements made on a headphones prototype.

Keywords: headphones, ANC, hybrid control, psychoacoustics.

Introduction

Active Noise Control (ANC) headphones provide to the user an attenuation of the acoustical noise present in the environment. This protection is a mixed effect of the characteristics of the headphones' construction materials and the ANC applied to the noise that effectively enters the ear-cups. The passive attenuation produced by the materials is effective in the mid and high frequency ranges. The low frequency range is actively treated using ANC, by generating sound waves through the headphone's speaker, such that the environmental noise is canceled out by superposition.

Generally, ANC headphones are equipped as shown in Fig. 1. A reference microphone outside the ear-cup measures the incident noise $x(n)$. The noise travels further through the ear-cup and reaches the position of the error microphone as $d(n)$. Thus, the transfer function $P(z)$ represents the influence of the headphone's materials and the relative position of the noise source to the system. The control signal $y'(n)$ is sent to the headphone's speaker and transformed into $y(n)$ by the transfer function $S(z)$. This transfer function represents the influences of the speaker and the acoustic path between the speaker and the error microphone. Finally, the acoustic signals $y(n)$ and $d(n)$ overlap destructively and lead to the residual error $e(n)$ at the position of the error microphone.

ANC solutions that use $x(n)$ for generating $y'(n)$ are called feedforward approaches, while the ones that use $e(n)$ instead are denoted as feedback approaches. Feedforward solutions based on adaptive filter techniques make also use of $e(n)$ as input for the adaptation algorithm [1]. Adaptive feedback solutions make only use of $e(n)$.

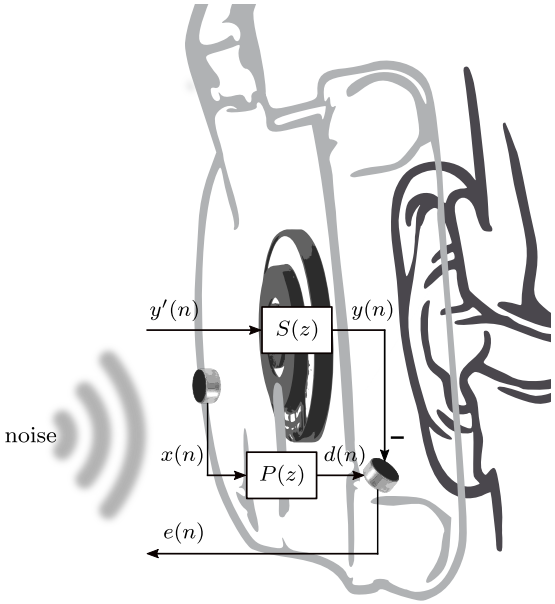

Figure 1: General description of signals and systems related to an Active Noise Control Headphone.

The combination of feedforward and feedback approaches into a hybrid structure provides the possibility to combine the performance of the single control structures into one and compensate for their individual limitations. A very attractive feedback approach for this purpose is the Minimum Variance Controller (MVC) [2], mainly because it is a low-order filter and it effectively attenuates low frequencies up to 1 kHz. The combination of an MVC with a feedforward controller [3][4][5][6][7] leads to a change in the effective secondary path seen from the feedforward sub-structure's perspective. This can be problematic, if it is not taken into account when using an adaptation algorithm like the FxLMS. Nevertheless, it is found that the later is effectively circumvented by the strategy proposed by Foudhaili in [8], called *Feedback-Feedforward-Kombination mit Substraktion der adaptiven Steuergröße*. This hybrid structure introduces instead a dependency between the feedforward controller's optimal solution and the feedback controller.

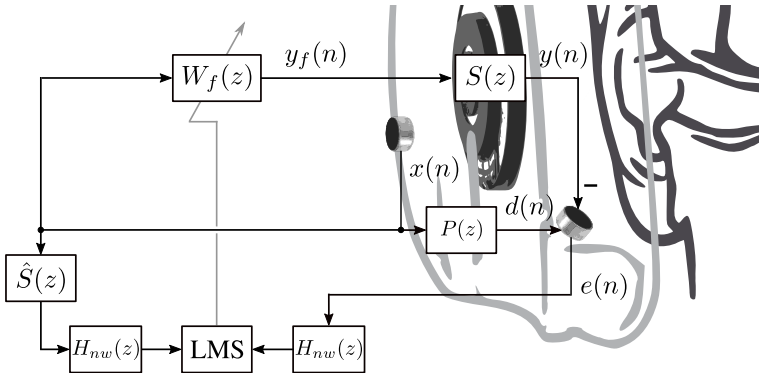

Figure 2: System diagram of the perceptually motivated adaptive feedforward structure [9].

In this work, the perceptually motivated feedforward FeLMS structure proposed by Bao in [9] (presented in Fig. 2 as a reference) is extended with a digital MVC substructure into a hybrid system by following the connection strategy of Foudhaili. The advantage of Bao's structure, in comparison to

a classical adaptive feedforward structure based on the FxLMS algorithm, relies on the psychoacoustic weighting of both signals used for the adaptation algorithm using the ITU-R 468 noise weighting (shown as $H_{nw}(z)$ in Fig. 2). This results in a system that attenuates the frequencies to which the human ear is more sensitive [10] with higher priority than the rest. Although the structure reduces the perceived loudness and increases the pleasantness (defined and named as *Wohlklang* by Aures in [11]) of the residual noise, it leaves the low frequencies almost unaltered. This leaves space for the MVC to provide the system with further attenuation of the residual noise that could not be attenuated by the feedforward scheme.

In the following section, the resulting hybrid structure is presented and its transfer function is derived. In the subsequent section the experimental setup is described together with the implementation parameters used for programming the system into an FPGA-based headphones prototype. Afterwards, measurements are conducted by means of a dummy-head wearing the prototype and an evaluation in frequency domain and by using psychoacoustic metrics is conducted, in order to estimate the improvement in the perceived pleasantness of the residual noise. Finally, conclusions are drawn based on the comparison between the proposed hybrid system and the system proposed by Bao.

The Hybrid Structure

The proposed hybrid structure presented in Fig. 3 is an extension of the feedforward structure shown in Fig. 2 with an MVC controller, by following the connections suggested by Foudhaili in [8]. The structure is designed to search the perceptually motivated optimal solution of $W_f(z)$ by means of the FeLMS algorithm and the ITU-R 468 noise weighting filter $H_{nw}(z)$, while the MVC controller attenuates the lower frequencies that can not be attenuated with the feedforward scheme. Here, the feedforward controller $W_f(z)$ uses the reference signal $x(n)$ to generate the control signal $y_f(n)$. This control signal is then added to $y_b(n)$, which is generated by the feedback controller $W_b(z)$, before they are played together through the headphone's speaker. In order to generate the input for the feedback controller, $y_f(n)$ is filtered by $\hat{S}(z)$ and then added to the error signal $e(n)$. This cancels the influence of $y_f(n)$ at the error microphone position, if $\hat{S}(z) = S(z)$ is chosen. The result of the addition is then an approximation of the residual error left by the feedback controller alone, which theoretically isolates the feedback controller from the influence of the feedforward controller.

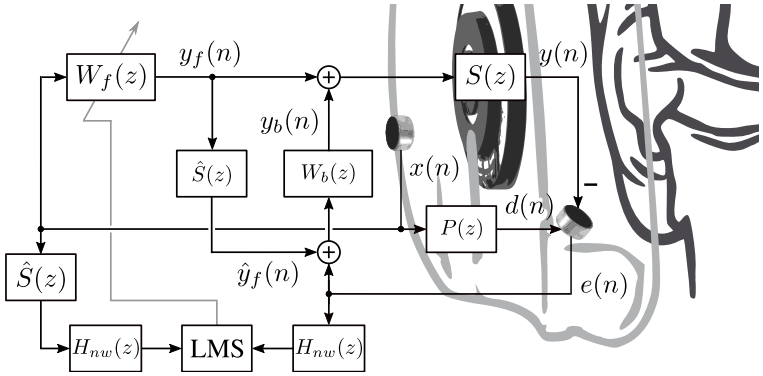

Figure 3: System diagram of the proposed perceptually motivated adaptive hybrid structure.

The effect of the interaction between both substructures as an ANC system is analyzed through its transfer function. For this, the equations that define the system

$$E(z) = D(z) - S(z) \cdot (Y_f(z) + Y_b(z)), \quad (1)$$
$$D(z) = P(z) \cdot X(z), \quad (2)$$
$$Y_f(z) = W_f(z) \cdot X(z), \quad (3)$$
$$Y_b(z) = W_b(z) \cdot (E(z) + \hat{Y}_f(z)), \quad (4)$$

and

$$\hat{Y}_f(z) = \hat{S}(z) \cdot W_f(z) \cdot X(z) \tag{5}$$

are required. By using (5) to replace $\hat{Y}_f(z)$ in (4), the resulting equation can be used together with (3) to replace $Y_b(z)$ and $Y_f(z)$ in (1). The resulting definition of $E(z)$ as a function of the reference signal $X(z)$ can be written as the transfer function given by

$$\frac{E(z)}{X(z)} = \frac{P(z) - S(z) \cdot W_f(z) \cdot (1 + \hat{S}(z) \cdot W_b(z))}{1 + S(z) \cdot W_b(z)}. \tag{6}$$

It can be seen that the denominator of this expression is the same as the denominator in the MVC's transfer function $1/(1 + S(z)W_b(z))$. So, if $W_b(z)$ is correctly designed, such that it yields a stable closed-loop system, then the stability of the hybrid system relies on the correct and stable adaptation of the controller $W_f(z)$. The adaptation of $W_f(z)$ may face stability issues, if strong differences between $S(z)$ and $\hat{S}(z)$ are to be found. This could cause that the optimal solution yields a control signal with an amplitude beyond the limits of the platform, as a side-effect of the strong coloration introduced by the term $(1 + \hat{S}(z) \cdot W_b(z))/(1 + S(z)W_b(z))$. In order to avoid such a scenario, a combination of a leaky-FeLMS algorithm together with a triggered on-line re-estimation of the system $S(z)$ could be used. If the estimation of $S(z)$ is correct, then $\hat{S}(z) = S(z)$ hold, and (6) results in the transfer function

$$\frac{E(z)}{X(z)} = \frac{P(z)}{(1 + S(z) \cdot W_b(z))} - S(z) \cdot W_f(z). \tag{7}$$

Looking at the left term in the subtraction, it can be seen that $P(z)$ is multiplied by the transfer function $1/(1 + S(z)W_b(z))$ of the MVC controller $W_b(z)$. Now, the optimal solution of $W_f(z)$ does not only consist of $S(z)$ and $P(z)$ as parameters, but also $W_b(z)$. This is understood as the dependency of the feedforward scheme's optimal solution on the feedback loop.

Experimental Setup

The overview of the experimental setup is presented in Fig. 4. A Neumann KU100 dummy-head is placed inside a room designed for audio-listening with dimensions 4.80 m x 4.20 m x 2.0 m. At a 1 m distance from the dummy-head's left side, a Genelec 8030B speaker is placed. The speaker is connected to an RME Fireface UC audio interface (bottom front), which is used to generate the excitation signals for the measurements and to record by means of the dummy-head at a sampling frequency of 48 kHz. An ANC headphone prototype based on a Beyerdynamic DT 770 PRO headset customized with inner and outer electret microphones on its ear-cups is utilized as system under test. Preamplifiers with a gain of 20 dB are used to better match the expected dynamic range of the microphones signal with the ± 10 V input range of the dSpace FPGA-based real-time platform. Additional to that, a Behringer Powerplay Pro-8 headphones power amplifier is used.

The excitation used is a Gaussian white noise signal amplitude-modulated with a modulation frequency of 70 Hz and a modulation degree of 30%, in order to generate some degree of roughness as used in [9]. The SPL of the signal measured at the right ear's position is 82.31 dB.

A 2048-samples-long impulse response of the secondary path, $S(z)$, is measured beforehand using the method proposed in [12] and used as $\hat{S}(z)$ in the evaluated control schemes. Fixed-point VHDL implementations of the structures to be evaluated running at a sampling frequency of 48 kHz are programmed, by following the filtering strategy suggested in [13]. The length of the adaptive FIR filter used for $W_f(z)$ is chosen to be equal to 1024 samples with a word-length of 64 bits, from which 48 bits are dedicated for the decimal part. The step-size $\mu_f = 2 \cdot 10^{-12}$ for the adaptive algorithms is chosen after a manual iteration on the trade-off between adaptation speed and stability.

Around the control structures, programmable control logic is used to bypass $H_{nw}(z)$, if required, also start and stop the adaptation algorithm, and to reset the filter coefficients. Additionally, the

MVC controller can be disconnected from the scheme, for the cases in which only the feedforward substructure is required for the evaluation.

Figure 4: Overview of the experimental setup used for the evaluation.

Evaluation

In order to evaluate the hybrid structure and to establish how it performs in comparison to the systems presented in [9], the measurement setup previously described is used. The control logic in the platform is parameterized so that first the classical feedforward FxLMS structure without psychoacoustic weighting $\mathrm{FF}_{\mathrm{flat}}$ is set. The system adapts during 5 min under the excitation of uniformly distributed white noise and afterwards the adaptation is stopped. Then the excitation signal is changed to the amplitude-modulated Gaussian white noise already described in the previous section and a 14 s recording is made by means of the dummy-head's left ear. This procedure is repeated with the feedforward FeLMS structure with psychoacoustic weighting $\mathrm{FF}_{\mathrm{psy}}$ and finally with the proposed hybrid structure $\mathrm{Hyb}_{\mathrm{psy}}$. An additional recording is done when no ANC is applied, in order to have a reference of the noise that effectively enters the ear-cup and reaches the dummy-head's left ear. The recorded signals are divided into 8192 samples-long non-overlapping frames, which are windowed with a Hamming window before their FFTs are calculated. The resulting spectra are time-averaged over the 14 seconds and presented as single-sided magnitude versus frequency plots in the 20 Hz to 20 kHz frequency range.

The results obtained are summarized in Fig. 5. By comparing $\mathrm{FF}_{\mathrm{flat}}(f)$ with $\mathrm{Off}(f)$ an attenuation bandwidth approximately between 60 Hz and 7500 Hz with non uniform attenuation values is to be found. Below 60 Hz and down to 20 Hz an amplification is produced, probably due to the small impact of this narrow frequency range on the overall optimal solution, compared to the total range of frequencies over which the filter is optimized. Beyond 7500 Hz the $\mathrm{FF}_{\mathrm{flat}}(f)$ produces no significant effect. If $\mathrm{FF}_{\mathrm{flat}}(f)$ is used as a reference for the evaluation of the behavior shown by $\mathrm{FF}_{\mathrm{psy}}(f)$, the influence of the psychoacoustic weighting can be seen. Thus, frequencies below approximately 650 Hz are not significant for the optimal solution anymore and almost no attenuation is generated in that range. Furthermore, improvements in the attenuation values can be seen up to 6 kHz. In disregard of the psychoacoustic weighting, an amplification peak is generated at 6300 Hz[1]. This artifact may

[1]The artifact may cause instability, if a bigger step-size μ is used

come from a discrepancy between $S(z)$ and $\hat{S}(z)$ or from the psychoacoustic weighting implementation. The same artifact appears again in the control structure Hyb_{psy}, which appears to combine the attenuation capabilities of the FF_{psy} in the higher frequencies with a substantially better attenuation in the lower frequencies up to 300 Hz. Thus, it provides a significant attenuation in the first 40% of the human hearing range, which is not addressed with psychoacoustic weighting. An interesting observation is that the feedback and feedforward substructures in Hyb_{psy} almost do not influence each other, because of the spectral distance that exists between the end of the MVC's attenuation band (300 Hz) and the beginning of the attenuation band of the feedforward controller (650 Hz). Thus, the solution of the feedforward substructure does not substantially deviate from its optimum, when the feedback controller is incorporated.

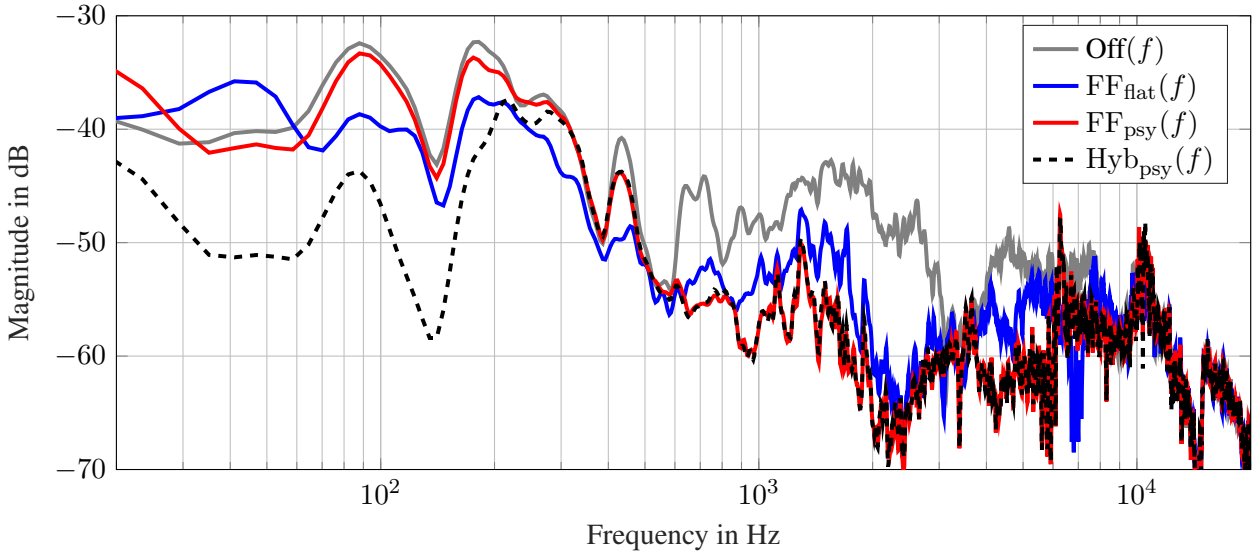

Figure 5: Signal spectra measured at the KU100 dummy-head's right ear under four different scenarios: Off(f), when no ANC is applied; FF_{flat}, when classical adaptive feedforward control is applied; FF_{psy}, when adaptive feedforward control with psychoacoustic weighting (ITU-R 468) is applied; and Hyb_{psy}, when adaptive hybrid control with psychoacoustic weighting (ITU-R 468) is applied. In all cases an adaptation time of 5 min and a $\mu = 2 \cdot 10^{-12}$ are used.

Additionally to the analysis presented before, a psychoacoustic evaluation of the recordings is conducted with the *NI Sound and Vibration Measurement Suite* of LabVIEW®, which uses the metric definitions proposed in [11]. The results are summarized in Fig. 6. In order to provide a reference, a recording performed with the dummy-head without headphones is also added next to the prior evaluated cases. Please note that, because the excitation signal and the residual error do not contain any tonal component, the resulting tonality is found to be zero for all studied cases and therefore not included in the plots.

By looking at the first row of results in Fig. 6, the first thing that can be noticed is that the passive damping of the headphones materials produces already a significant noise reduction. The reduction is reflected into a significant drop in the loudness and sharpness, which consequently increases the overall pleasantness. In Fig. 6(b), it can be seen that all three ANC structures lead to a further significant loudness reduction in comparison to the passive headphones (more than 5 sone). Furthermore, the hybrid MVC structure results in a slightly lower loudness compared to the two feedforward structures, due to the additional attenuation of the lower frequencies provided by the feedback controller. In Fig. 6(d) it can be noticed that the increase in the system's complexity produces a comparable decrease of the roughness, which consequently generates an increment in pleasantness. As a result, the proposed adaptive hybrid structure leads to the highest pleasantness value among the evaluated systems.

Although between FF_{psy} and Hyb_{psy} the differences in loudness, sharpness and resulting pleasantness are small, a study of the Just Noticeable Difference (JND) of these metrics for the specific application on ANC headphones is still missing in the literature. For example, in [14] JNDs of loudness, sharpness, and roughness for refrigerator noise were found to have values of 0.5 sone, 0.08 acum, and 0.04 asper, respectively.

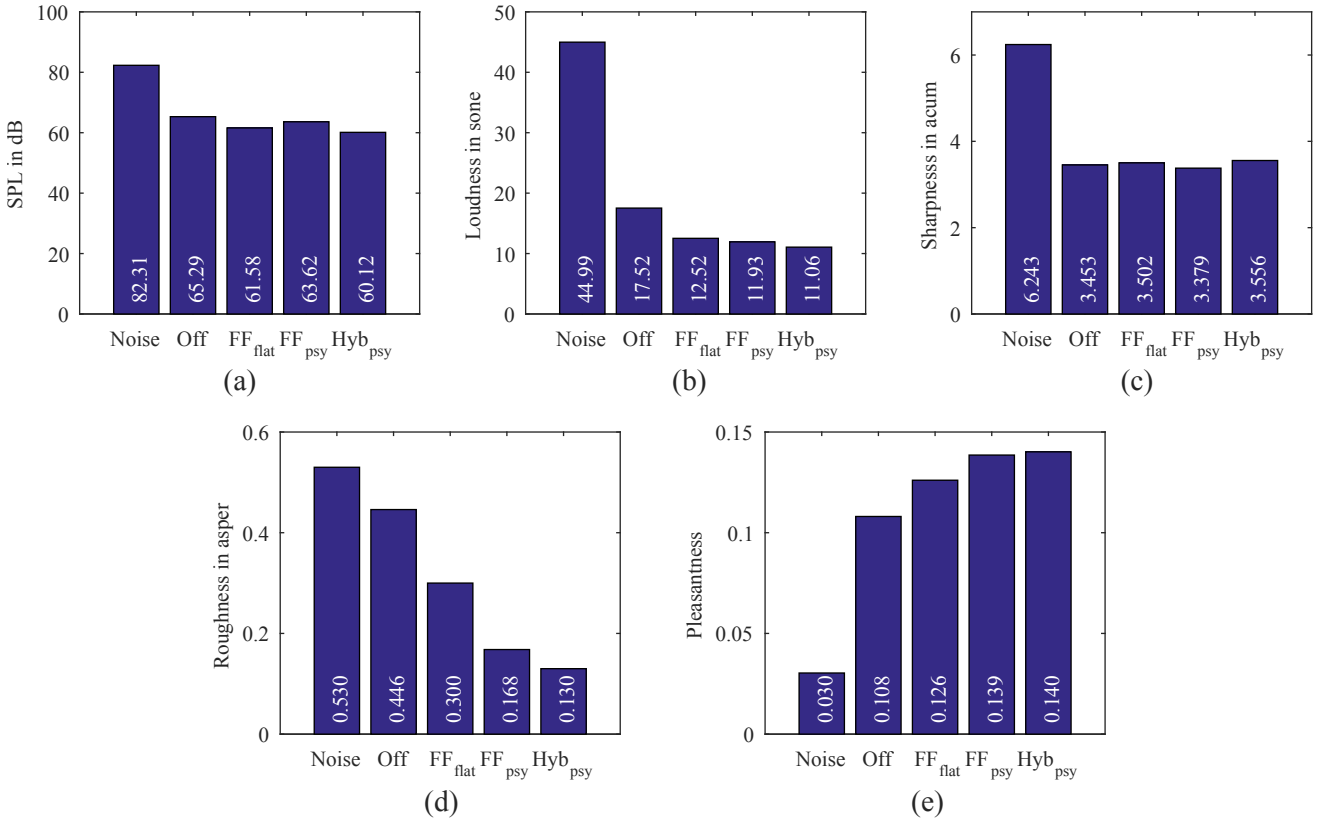

Figure 6: Psychoacoustic objective metric results under white gaussian noise amplitude-modulated with a modulation frequency of 70 Hz and a modulation degree of 30%. Noise, when the dummy-head is wearing no headphones; Off, when the dummy-head is wearing the headphones, but no ANC is applied; FF_{flat}, when classical adaptive feedforward control is applied; FF_{psy}, when adaptive feedforward control with psychoacoustic weighting (ITU-R 468) is applied; and Hyb_{psy}, when adaptive hybrid control with psychoacoustic weighting (ITU-R 468) is applied. In all cases an adaptation time of 5 min and a $\mu = 2 \cdot 10^{-12}$ are used

Conclusions

In this work an adaptive hybrid control structure is proposed to partially compensate the limitations of a perceptually motivated adaptive feedforward structure. For a realistic evaluation, a real-time FPGA implementation of the control algorithms is connected to an ANC headphones prototype. The evaluation of the measurement results shows that the passive attenuation provided by the headphones materials plays a dominant role in the pleasantness of the overall system. Nevertheless, the implemented ANC structures contribute to a further reduction of loudness and roughness. Among the evaluated control structures, the proposed structure shows the best results in attenuation and objective metrics, which is consistent with the qualitative pleasantness experienced when using the prototype. Because of the important role that the estimated secondary path plays in this structure, a triggered online re-estimation of it should be evaluated in a future work, in order to ensure stability and optimal attenuation values.

REFERENCES

1. Sayed, A. H., *Fundamentals of Adaptive Filtering*, Wiley-IEEE Press, 1 edn. (2003).
2. Pawełczyk, M. Analogue active noise control, *Applied Acoustics*, **63** (11), 1193–1213, (2002).
3. Johansson, S., Winberg, M., Lagö, T. and Claesson, I. A New Active Headset For a Helicopter Application, *1997 Proceedings of the 5th International Congress on Sound and Vibration*, December, (1997).
4. Carme, C. The third principle of active control: The feed forback, *INTER-NOISE and NOISE-CON Congress and Conference Proceedings*, **1999** (5), 885–896, (1999).
5. Rafaely, B. and Jones, M. Combined feedback-feedforward active noise-reducing headset–the effect of the acoustics on broadband performance, *The Journal of the Acoustical Society of America*, **112** (3), 981–989, (2002).
6. Streeter, A. D., Ray, L. R. and Collier, R. D. Hybrid feedforward-feedback active noise control, *Proceedings of the 2004 American Control Conference*, June, vol. 3, pp. 2876–2881 vol.3, (2004).
7. Wu, L., Qiu, X., Burnett, I. S. and Guo, Y. Decoupling feedforward and feedback structures in hybrid active noise control systems for uncorrelated narrowband disturbances, *Journal of Sound and Vibration*, **350**, 1 – 10, (2015).
8. Foudhaili, H., *Kombinierte feedback- und adaptive Feedforward-Regelung für aktive Lärmreduktion in einem Kommunikations-Headset*, Ph.D. thesis, Leibniz Universität Hannover, Aachen, (2008).
9. Bao, H. and Panahi, I. A perceptually motivated active noise control design and its psychoacoustic analysis, *ETRI Journal*, **35**, 859–868, (2013).
10. Fastl, H. and Zwicker, E., *Psychoacoustics: Facts and Models*, Springer-Verlag New York, Inc., Secaucus, NJ, USA (2006).
11. Aures, W., *Berechnungsverfahren für den Wohlklang beliebiger Schallsignale, ein Beitrag zur gehörbezogene Schallanalyse*, Ph.D. thesis, Technische Universität München, München, (1984).
12. Rivera Benois, P., Bhattacharya, P. and Zölzer, U. Derivation technique for headphone transfer functions based on sine sweeps and least squares minimization, *Proceedings of the 45th International Congress and Exposition on Noise Control Engineering, INTER-NOISE*, Aug, (2016).
13. Rivera Benois, P., Nowak, P. and Zölzer, U. Fully Digital Implementation of a Hybrid Feedback Structure for Broadband Active Noise Control in Headphones, *2017 Proceedings of the 24th International Congress on Sound and Vibration*, July, (2017).
14. J., Y. and J.Y., J. Just noticeable differences in sound quality metrics for refrigirator noise, *Noise Control Engineering Journal*, **56** (6), 414–424, (2008).